lubricants

Article

Optimization of the Tribological Performance and Service Life of Calcium Sulfonate Complex—Polyurea Grease Based on Unreplicated Saturated Factorial Design

Hong Zhang [1,*], Yimin Mo [1], Qingchun Liu [1], Jun Wang [2] and Qian Li [2]

[1] School of Mechanical and Electrical Engineering, Wuhan University of Technology, Wuhan 430070, China
[2] SAIC GM-Wuling Automobile Co., Ltd., Liuzhou 545007, China
* Correspondence: hongybyb@163.com

Abstract: In order to further extend the service life of calcium sulfonate complex–polyurea grease (CSCPG) while ensuring its tribological performance, this article starts with the production of raw materials and the preparation process of the grease and explores the factors that significantly affect the tribological performance and service life of CSCPG based on unreplicated saturated factorial design (USFD). The Kriging prediction model is used along with the optimization objectives of friction coefficient and service life, and nondominated sorting genetic algorithm II (NSGA-II) was used for a multi-objective optimization solution. The tribological and service life tests were conducted before and after optimization. The results show that the viscosity of the base oil and the content of the nano-solid friction reducers have a significant impact on the tribological properties of CSCPG. The content of polyurea thickeners and antioxidants, as well as the thickening reaction temperature, have a significant impact on the service life of CSCPG. When the friction coefficient and service life are optimized as objectives and are compared to the initial group, the friction coefficient of CSCPG could be reduced by 5.3%, and the service life could be extended by 3.8%. The Kriging prediction model based on USFD has high accuracy and can be used to guide the preparation and performance optimization of CSCPG.

Keywords: calcium sulfonate complex-polyurea grease; tribological performance; service life; unreplicated saturated factorial design

check for updates

Citation: Zhang, H.; Mo, Y.; Liu, Q.; Wang, J.; Li, Q. Optimization of the Tribological Performance and Service Life of Calcium Sulfonate Complex—Polyurea Grease Based on Unreplicated Saturated Factorial Design. *Lubricants* **2023**, *11*, 377. https://doi.org/10.3390/lubricants11090377

Received: 17 August 2023
Revised: 31 August 2023
Accepted: 4 September 2023
Published: 5 September 2023

1. Introduction

Bearings are the core supporting components of rotating machinery. With the popularization of ultra-precision machining technology in the field of bearing processing, surface roughness and machining accuracy are no longer the main factors restricting bearing quality. More bearing failures are caused by lubrication failures, and bearing lubrication has gradually become a key factor in the reliability and efficiency of mechanical systems [1]. Therefore, how to improve bearing lubrication status to reduce bearing friction and extend bearing life while meeting the requirements of various extreme working conditions has significant theoretical significance and engineering application value.

The thickening agent system of calcium sulfonate complex grease (CSCG) mainly consists of two parts [2,3]. One part is non-Newtonian overbased petroleum calcium sulfonate, in which calcium carbonate exists in the form of calcite crystals and is encapsulated by a certain concentration of calcium sulfonate to form stable micelles [4]. The other part is composite calcium soap (including fatty acid calcium, borate calcium, etc.), which together form a relatively complex thickening agent system, giving CSCG excellent high- and low-temperature performance, oxidation stability, and lubrication performance [5]. Research has shown that CSCG has a more stable friction coefficient and higher wear resistance when compared to commercial lithium greases [6], and better thermal stability and a higher high-temperature bearing capacity when compared to composite lithium greases [7]. Therefore, in recent years, CSCG has been widely used in bearing lubrication, especially in high-temperature greases, showing unique vitality.

Calcium sulfonate thickener can form a boundary friction film composed of $CaCO_3$, CaO, iron oxide, and $FeSO_4$ on the friction surface [8], which is an important reason for the great wear resistance of CSCG. However, Gao, Y [9] compared the tribological behavior of CSCG and polyurea grease via SRV (Schwingung, Reibung, Verschleiss) experiments and found that CSCG had poorer friction-reducing performance than the latter. Therefore, many researchers have used nano-solid friction reducers to improve the tribological properties of CSCG. WS_2 nanoparticles can effectively reduce the friction coefficient of lubricating grease, which is mainly attributed to the adsorption and frictional chemical reactions between WS_2 nanoparticles and the matrix [10]. Multiple combinations of nanoparticles are added to CSCG (such as the combination of hexagonal boron nitride and nano-Al_2O_3 [11] or the combination of MoS_2, CuO, SiO_2, and Al_2O_3 nanoparticles [12]). This can not only improve the tribological performance of CSCG but also suppress bearing vibration. The tribological and rheological properties of polyurea greases depend on both the viscosity of the base oil [13,14], and the structure of the used amine [15,16] tetraurea with a granular structure presents optimal physicochemical properties and structural strength; the diurea grease with a rodlike structure presents the optimal tribological properties [17], and its excellent lubrication properties mainly depend on the synergistic effect of the lubricating grease film and the chemical reaction film [18].

The service life of lubricating grease directly affects the service life of bearings. Lubricating grease not only provides lubrication protection for bearings but also serves as a seal to prevent water from entering the bearings [19]. CSCG can be widely used in humid environments due to its unique water absorption performance. CSCG contaminated by water can generate a uniform water calcium sulfonate thickener micelle structure [20,21]. However, during the friction process, water can have an impact on the film-forming ability and film thickness of CSCG [22]. Cyriac, F [23] found that the effect of water on elastohydrodynamic lubrication film thickness is related to oil leakage. Unlike lithium grease and polyurea grease, the oil leakage of CSCG decreases after being contaminated with water, leading to an increase in starvation. When compared with uncontaminated grease, the film is thinner.

Experiments based on a factorial design can screen for significant influences among a large number of possible factors, and unreplicated factorial design experiments tend to be saturated when a large number of factors are considered. The USFD method [24,25] requires fewer tests in the factorial design, and a larger number of factors can be examined, which saves both test time and test costs. The Kriging prediction model [26] is an unbiased estimation model that predicts responses for unknown points based on known sample point information. This model converts the positional relationship between sample points in space into a variance relationship and performs an optimal linear unbiased estimation of variables in a limited area. The established prediction model has high fitting accuracy in highly nonlinear situations. NSGA-II [27,28] is an improved version of NSGA, which uses a fast, nondominated sorting technique and the crowding principle to solve the problems of NSGA, such as the complexity being too high and the excellent individuals not being easy to select in the iterative process, which has the advantages of good solution convergence and a fast running speed.

Indeed, significant progress has been made in previous research on the tribological properties and service life of CSCG after water absorption. However, there are still some issues that need further research, such as the poor sensitivity of CSCG to nano-solid friction reducers, and there is relatively little research on how to balance the lubrication performance and service life of CSCG. In response to the above issues, this study started with the production of raw materials and preparation process for lubricating grease and introduced organic polyurea compounds into CSCG to prepare calcium sulfonate complex–polyurea grease (coded CSCPG). Based on USFD, the factors that significantly affect the tribological performance and service life of CSCPG were explored, and a Kriging prediction model of

CSCPG was established to optimize the friction coefficient and service life. NSGA-II was used for multi-objective optimization solutions, and the performance of the lubricating grease before and after optimization was compared through tribological tests and life tests. The research work can provide a theoretical and experimental basis for the preparation and optimization of high-temperature lubricating grease.

2. Design and Preparation

2.1. Preparation of CSCPG

As shown in Figure 1, the preparation process of CSCPG is as follows: Firstly, the overbased calcium sulfonate T106A (the total base number ≥ 395 mgKOH/g) and water accounting for 10~20% of the total weight of the overbased calcium sulfonate are added to a reactor containing the base oil for mixing; this is stirred evenly and heated to 80 °C. Then, add the transforming agent (ethylene glycol monomethyl ether) to the reactor and stir evenly; the conversion is carried out at T_1 = 90 °C, the conversion time is t_1 = 60~90 min, and the temperature is controlled at T_2 = 95~100 °C. After that, the saponification reaction is carried out by adding saponification agents (fatty acid, boric acid), and the saponification time is t_2 = 60 min. Then, control the temperature T_3 = 90~100 °C, add the polyurea thickener (diisocyanate, toluidine) to the above reaction kettle for a constant temperature reaction of t_3 = 90 min, rapidly cool to below T_4 = 80 °C, add nano-solid friction reducers (WS_2 nanoparticles) and antioxidant agent (dialkyl diphenylamine) and stir for t_4 = 30 min to mix the additives and lubricating grease evenly. Finally, grind with a three-roller mill grinder to obtain the finished lubricating grease.

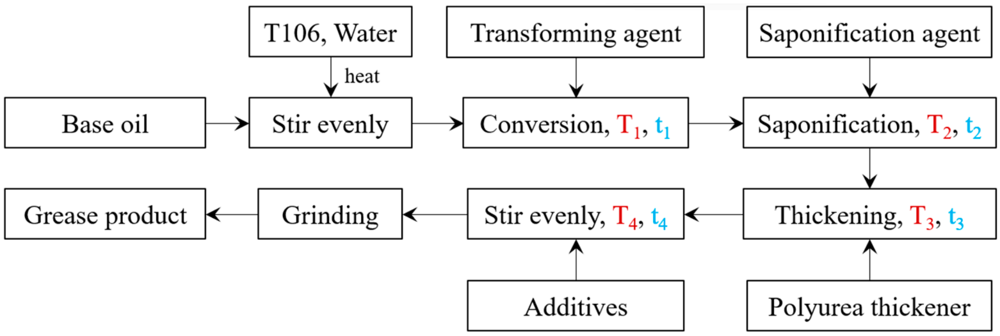

Figure 1. Preparation flowchart of CSCPG.

2.2. Unreplicated Saturated Factorial Design

From Figure 1, the preparation of CSCPG encounters problems, such as multiple types of raw materials, complex processes, and multiple control points. There may also be mutual influences among the various factors. Even if the raw materials are completely the same, CSCPG batches that have different performances will be prepared due to different process flows. However, the optimization of a single factor often cannot meet the demand for improving the performance of lubricating grease, and it is impossible for all factors to have a significant impact on the performance of lubricating grease. Therefore, it is of great significance to deeply explore the key influencing factors of CSCPG performance. Here, the USFD method is used to identify the significant influencing factors on the performance of CSCPG using as few experiments as possible. The following statistical model is used to describe this problem.

$$y_j = \sum_{i=0}^{p} x_{ji}\beta_i + \varepsilon_j \; j = 1, \cdots, n \quad (1)$$

In Equation (1):

(1) $y = (y_1, \ldots, y_n)^{\mathrm{T}}$ is the observation vector, and n is the number of experiments;
(2) β_i, $i = 0, \ldots, p$ is an unknown set of significant influencing factor parameters, β_0 is the general average, and they are all parameters to be estimated, $p = n - 1$;

(3) $x_i = (x_{1i}, x_{2i}, \ldots, x_{ni})^T$ is an orthogonal design matrix, with the column vectors x_0, x_1, …, x_p being known, $x_0 = 1_n$ being n-dimensional column vectors with all elements 1, $x_1, \ldots, x_p$ determined by the experimental design;
(4) $\varepsilon = (\varepsilon_1, \ldots, \varepsilon_n)^T$ is the error vector and assumes: ε_i, $i = 1, \ldots, n$ are independent random variables with the same mean of 0 and the same variance σ^2, ε_i follows a normal distribution, i.e., $\varepsilon \sim N(0, \sigma^2 I_n)$; there are, at most, $r(1 \leq r < p)$ factors with nonzero effects among the p factors, i.e., at most, the r of $\beta_1, \ldots, \beta_p$ are not equal to zero.

The purpose is to use n observation values $y_1, \ldots, y_n$ to observe whether there is a significant effect among the p effects. That is, to test the following assumptions:

H_0. *$\beta_1 = \beta_2 = \ldots = \beta_p = 0$.*

H_1. *β_i is not all zero.*

If H_0 is rejected, this indicates the presence of significant factors, and then we determine which factors are significant.

2.3. Tribological Performance Test

The tribological properties of the prepared lubricating grease were studied using an MFT-5000 friction testing machine (Rtec Instruments, San Jose, CA, USA) (Figure 2a). The friction pair samples used in the experiment included AISI E52100 steel (Figure 2b) and Si_3N_4 balls with a diameter of 7 mm. The Si_3N_4 ball was fixed on the loader and loaded vertically. The overall size of the AISI E52100 steel sample was 14 mm × 12 mm × 6 mm. We polished the surface of the sample with 1200 # and 2000 # sandpaper for 30 min on a polishing machine to ensure that the surface roughness parameters (the arithmetic mean Sa and root mean square Sq of the absolute value of contour offset) of the sample were less than 0.03 µm (Figure 2b). Finally, we cleaned the sample with alcohol ultrasonic for 10 min, applying a 2 mm thick lubricating grease sample evenly on the surface of the cleaned AISI E52100 steel sample with a ceramic spoon. We then fixed it to a reciprocating moving platform. The test conditions are shown in Table 1. As the moving platform moved horizontally, the real-time values of friction force and load were collected by the sensors of the friction testing machine, with a collection frequency of 100 values per second. We took the average value of the segments as the experimental result of the friction coefficient.

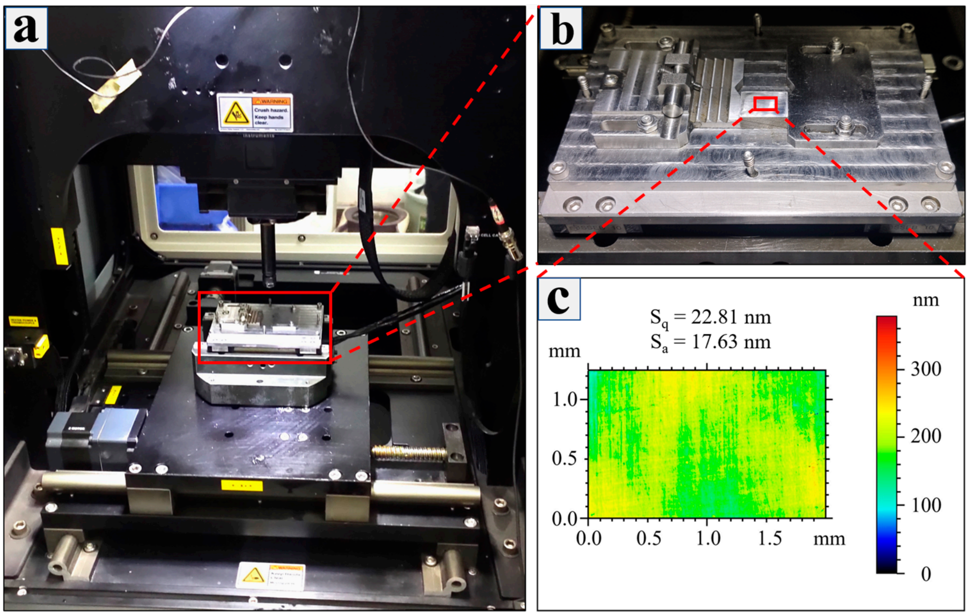

Figure 2. MFT-5000 friction and wear testing machine. (**a**) Testing machine body; (**b**) tested sample; (**c**) surface topography and the values of the basic surface roughness parameters of the sample.

Table 1. Test conditions for tribological test.

Reciprocating Distance/mm	Reciprocating Frequency/Hz	Test Load (Fz)/N	Test Time/min
8	1	20	30

After the friction test, the surface morphology of the wear marks was observed using a three-dimensional optical profilometer (UP-3D Rtec, Rtec Instruments, Silicon Valley, San Francisco, CA, USA), and the wear rate (W, $mm^3n^{-1}m^{-1}$) and amount of wear (V, mm^3) of the sample were analyzed. The formula for the amount of wear was as follows: $V = A \times L$. Among them, the cross-sectional area (A, mm^2) of the wear marks was calculated using a profiler, and each sample was measured 10 times. The average of the 10 measurements was taken as the result. The length of the wear marks (L, mm) was obtained by calculating the circumference of the friction test trajectory. The formula for wear rate was as follows: $W = V/(F \times S)$, where F (N) was the load and S (m) was the total friction distance.

2.4. Service Life Test

The lubrication service life of the prepared lubricating grease was tested using the FE9 Roller Bearing Wear Testing Machine. The test conditions shown in Table 2 refer to the DIN 51,821 standard, and the angular contact ball bearing 7206 was selected as the test bearing. Before the test, the lubricant in the bearing was cleaned with petroleum ether, and after, it was completely dried. The test lubricating grease was evenly filled into the bearing (the lubricating grease should not exceed the surface of the bearing ring) at a temperature of 25 °C and a speed of 1500 RPM. It was pre-run for 2 h under a load of 1500 N to evenly distribute the lubricating grease inside the bearing. When any one or more of the following situations occur in the bearing test, the lubricating grease is considered to have failed: (a) the input power of the main shaft is 300% of the stable value, (b) the temperature value of the outer ring of the bearing exceeds the stable value by 15 °C, (c) the test bearing is stuck or the belt is slipping, or (d) the operating torque of the main shaft is 500% of the stable value.

Table 2. Test conditions for service life test.

Axial Load/N	Bearing Speed/RPM	Temperature/°C
1500	6000	120

3. Multi-Objective Optimization Based on USFD

3.1. Experimental Design

As shown in Table 3, the factors that may affect the tribological properties and service life of lubricating grease during the preparation process of CSCPG are listed, including the proportion of three thickening agents [29]: overbased calcium sulfonate T106A (coded A), polyurea thickening agent (coded C), and composite calcium soap (coded D); base oil 40 °C kinematic viscosity (coded B) [14]; the proportion of the content of the two additives: antioxidant (coded E) [30] and nano-solid friction reducers [10–12] (coded F); reaction time: conversion reaction time T_1 (coded G), thickening reaction time T_3 (coded H); reaction temperature: conversion reaction temperature t_1 (coded J), thickening reaction temperature t_3 (coded K), and grinding gap (coded L) during post-treatment [31]. Table 3 also provides the range of values for each factor, where the initial value refers to the values of each factor before optimization, and the maximum and minimum values are the allowable range of values for each factor obtained based on experience.

Table 3. Initial values and value ranges of influencing factors.

Number	A/%	B/mm^2/s	C/%	D/%	E/%	F/%	G/min	H/min	J/°C	K/°C	L/mm
Initial value	26	150	8	4	2	1.5	90	100	90	130	0.2
Minimum	20	90	2	3	0.5	0.5	60	60	80	100	0.1
Maximum	35	300	10	6	3	2	120	120	100	130	0.4

From Table 3, the number of factors being considered has reached the maximum number of parameters that need to be estimated. Here, the estimated parameters refer to the parameters that can obtain their unbiased estimates. In order to minimize the number of experiments, the orthogonal saturated factorial design method and Plackett-Burman design were used to conduct n = 12 experiments on the selected p = 11 influencing factors. The friction coefficient is taken as the observation value 1 (coded y_1), the service life is taken as the observation value 2 (coded y_2), the droplet point is taken as the observation value 3 (coded y_3), and the cone penetration is taken as the observation value 4 (coded y_4). The experimental results are shown in Table 4; among them, "1" and "−1" represent the maximum and minimum values of the factor, respectively.

Table 4. Plackett-Burman design table and observations based on L_{12} (2^{11}).

No.	A	B	C	D	E	F	G	H	J	K	L	y_1	y_2	y_3	y_4
1	−1	1	1	−1	1	−1	−1	−1	1	1	1	0.14	240	316	278
2	1	1	1	−1	1	1	−1	1	−1	−1	−1	0.1	227	321	248
3	−1	−1	1	1	1	−1	1	1	−1	1	−1	0.11	239	318	256
4	1	1	−1	1	1	−1	1	−1	−1	−1	1	0.14	194	310	274
5	1	1	−1	1	−1	−1	−1	1	1	1	−1	0.13	191	322	260
6	−1	1	1	1	−1	1	1	−1	1	−1	−1	0.09	197	307	263
7	−1	−1	−1	1	1	1	−1	1	1	−1	1	0.07	193	298	286
8	1	−1	−1	−1	1	1	1	−1	1	1	−1	0.08	218	313	256
9	1	−1	1	1	−1	1	−1	−1	−1	1	1	0.08	215	326	253
10	1	−1	1	−1	−1	−1	1	1	1	−1	1	0.11	194	321	249
11	−1	1	−1	−1	−1	1	1	1	−1	1	1	0.09	195	306	289
12	−1	−1	−1	−1	−1	−1	−1	−1	−1	−1	−1	0.11	189	300	268

3.2. Screening of Significant Influencing Factors

In the above design, there are 12 sets of observations to estimate the 12 parameters to be estimated (including the general average β_0). There is no remaining degree of freedom to estimate the error variance; that is, the sum of the squared errors Se≡0, so it is not possible to use standard deviation analysis (F-test or *t*-test) for significance testing of influencing factors.

Here, the half-normal plot [32] method is used for the data processing of USFD. Under the assumption that the error is normal, independent, and of the same variance, the estimators of each factor are independent of each other. The estimators with zero influencing factors follow the same normal distribution, and their expected values are zero. On the half-normal plot, their observed values should be located on a straight line passing through the origin, whereas the expected values of the estimators with nonzero influencing factors should deviate from this straight line passing through the origin. As shown in Figure 3, by plotting the estimated values of each influencing factor on a half-normal plot, it is easy to identify the factors that have a significant impact on each observation. The results are summarized in Table 5.

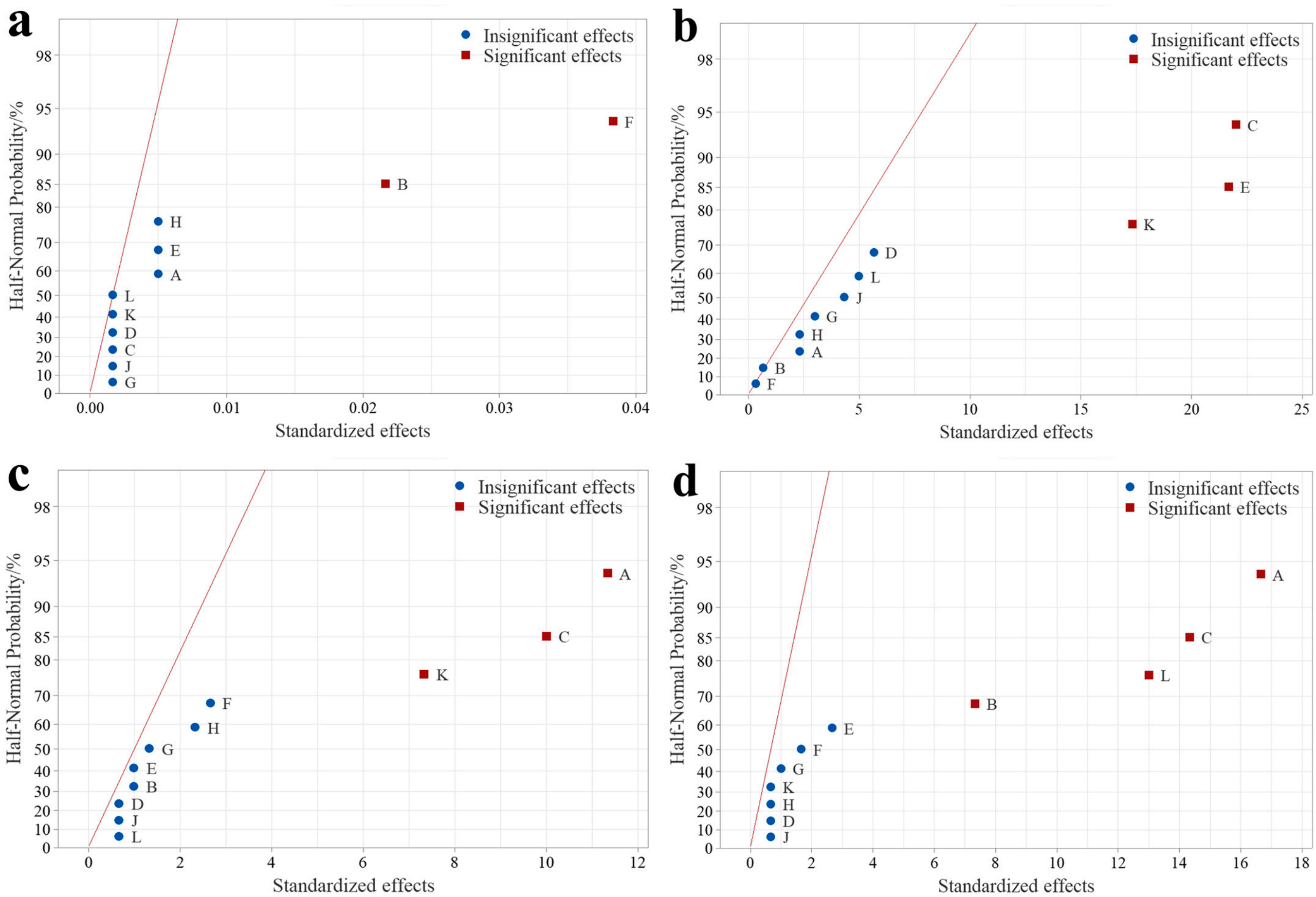

Figure 3. Half-normal plots of four observations. (**a**) y_1; (**b**) y_2; (**c**) y_3; (**d**) y_4.

Table 5. Significant influencing factors of four observations.

Observations	Significant Effects
y_1	B, F
y_2	C, E, K
y_3	A, C, K
y_4	A, B, C, L

3.3. NSGA–II Multi-Objective Optimization

From Figure 3 and Table 5, the main factors that have a significant impact on the friction coefficient and service life of CSCPG are the viscosity of the base oil, the proportion of polyurea thickeners, antioxidants, and nano-solid friction reducers, and the thickening reaction temperature T_3. Calcium sulfonate is the main component of CSCPG's thickening agent, which determines the basic performance of CSCPG. Therefore, the above six parameters are selected as design variables (Table 6), and a multi-objective optimization model

(Equation (2)) is established to optimize the tribological performance and service life of CSCPG, with y_1 and y_2 as the optimization objectives and y_3 and y_4 as the constraints.

$$
\begin{array}{ll}
\text{find} & (x_1, x_2, x_3, x_4, x_5, x_6) \\
 & \min \mathrm{y}_1, -\mathrm{y}_2 \\
\text{s.t.} & \mathrm{y}_3 \geq 300 \\
 & 244 \leq \mathrm{y}_4 \leq 294 \\
 & 20 \leq x_1 \leq 35 \\
 & 90 \leq x_2 \leq 300 \\
 & 2 \leq x_3 \leq 10 \\
 & 0.5 \leq x_4 \leq 3 \\
 & 0.5 \leq x_5 \leq 2 \\
 & 100 \leq x_6 \leq 130
\end{array} \tag{2}
$$

Table 6. Selection of design variables and their initial values.

Significant Factors	Design Variables	Initial Value
A	x_1	26
B	x_2	150
C	x_3	8
E	x_4	2
F	x_5	1.5
K	x_6	130

Due to the large number of design variables and their complex correlation, the optimal Latin hypercube design (OLHD) was used to randomly sample the design space. The OLHD improves the uniformity of the random Latin hypercube design, making all sampling points more evenly distributed in the design space, with excellent spatial filling and balance [33]. Then, the Kriging method is used to predict and model the design space. Table 7 shows 50 sets of sampling points and their observation values collected using the OLHD. The Kriging prediction model was established, as shown in Figure 4, with y_1 and y_2 as the design objectives and x_1~x_6 as the design variables.

Table 7. Sampling points and observation values based on OLHD.

No.	x_1	x_2	x_3	x_4	x_5	x_6	y_1	y_2	y_3	y_4
1	27	212	8	1.5	1	107	0.112	207	318	263
2	35	281	3	2	1.5	124	0.110	205	312	267
3	33	152	9	3	1.5	111	0.098	224	323	254
4	32	240	7	2	1	128	0.118	220	314	260
5	21	147	6	2	1.5	101	0.091	204	310	272
6	22	172	6	2.5	1	123	0.109	220	307	270
7	33	115	4	1	1	101	0.102	188	317	257
8	34	298	4	1.5	1.5	100	0.109	189	321	265
9	26	227	7	2.5	1.5	117	0.103	219	313	268
10	34	127	9	3	0.5	102	0.120	220	326	249
11	28	156	3	2.5	1.5	105	0.094	200	313	268
12	25	248	9	1.5	1.5	116	0.102	214	314	264
13	26	142	4	1	1	113	0.103	194	310	267
14	31	203	4	0.5	0.5	120	0.123	194	313	262
15	23	187	4	2	1.5	125	0.096	210	304	273
16	20	91	10	1	0.5	119	0.110	216	312	262
17	27	273	2	1.5	1	109	0.116	192	310	275
18	27	268	5	3	1	125	0.121	222	311	270
19	22	259	6	2	1.5	115	0.103	211	310	275
20	22	263	6	0.5	1	112	0.113	197	311	271

Table 7. *Cont.*

No.	x_1	x_2	x_3	x_4	x_5	x_6	y_1	y_2	y_3	y_4
21	31	136	8	2.5	1	121	0.108	223	318	255
22	27	122	8	2	1.5	112	0.091	214	315	260
23	31	170	8	2.5	0.5	126	0.124	226	315	258
24	34	211	10	2	0.5	108	0.128	215	327	250
25	23	183	9	1	2	107	0.081	206	313	263
26	32	194	2	1.5	0.5	129	0.124	202	309	267
27	33	245	5	1	1	127	0.116	204	313	262
28	24	118	5	1.5	1	122	0.101	209	308	267
29	24	129	7	0.5	2	106	0.074	196	311	264
30	34	235	5	1	2	105	0.089	192	320	262
31	21	294	10	1	1.5	128	0.106	221	310	268
32	32	254	3	2	1	130	0.119	210	309	267
33	30	256	9	0.5	2	103	0.089	198	323	259
34	28	159	7	2.5	2	106	0.083	211	314	262
35	33	110	8	1	2	108	0.076	203	320	253
36	20	176	8	1.5	1.5	122	0.093	215	309	270
37	30	101	7	1	1.5	117	0.088	204	314	256
38	24	279	6	2.5	1	114	0.120	213	311	272
39	29	104	4	2.5	2	103	0.077	201	312	266
40	29	220	3	1	1	126	0.113	199	309	270
41	25	207	5	1.5	2	115	0.084	204	308	271
42	28	182	4	2	0.5	117	0.122	206	312	267
43	29	98	9	3	0.5	121	0.118	230	316	256
44	22	198	7	0.5	1.5	129	0.095	210	308	267
45	25	230	2	3	0.5	110	0.128	206	308	276
46	30	290	8	2.5	1	111	0.124	217	319	263
47	25	287	3	2.5	1.5	119	0.108	208	307	278
48	29	163	3	2	2	118	0.083	203	308	268
49	21	221	5	1.5	1	104	0.110	197	309	275
50	23	137	6	1.5	1.5	113	0.090	205	309	269

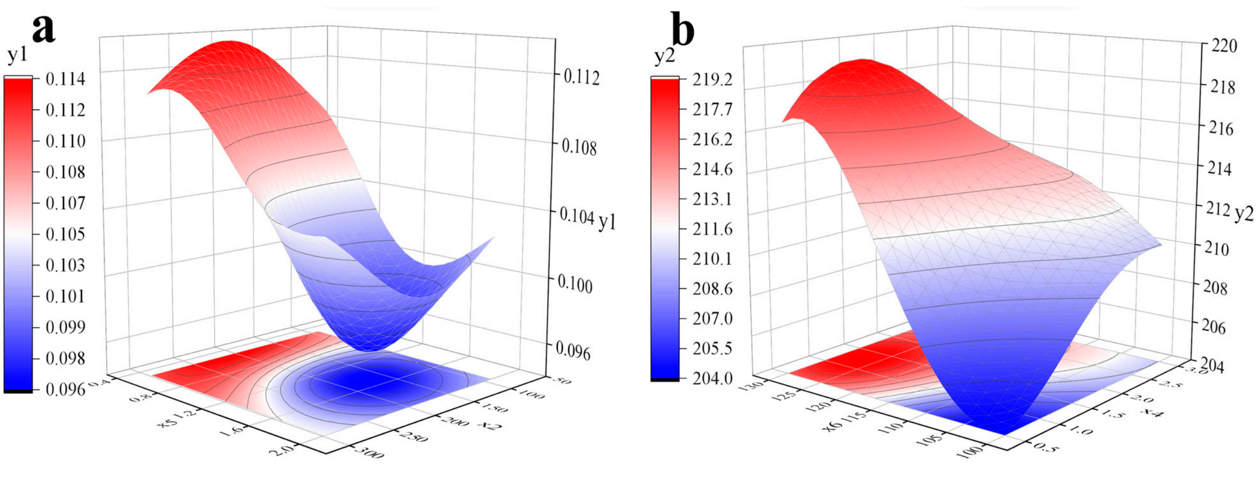

Figure 4. *Cont.*

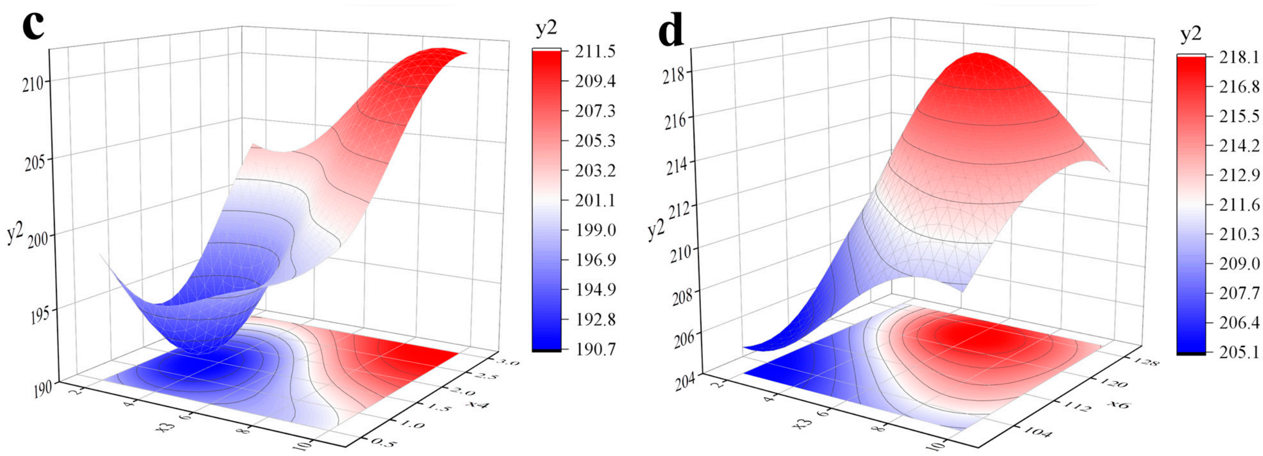

Figure 4. Kriging prediction model for friction coefficient and service life. (**a**) y_1 vs. x_2 and x_5; (**b**) y_2 vs. x_4 and x_6; (**c**) y_2 vs. x_3 and x_4; (**d**) y_2 vs. x_3 and x_5.

The accuracy error analysis of the constructed Kriging prediction model is shown in Table 8. The coefficient of determination R^2 and the corrected coefficient of determination $Radj^2$ of each Kriging prediction model exceeds 0.9, with a maximum error MRE of less than 0.1, indicating that the model has high accuracy and can be used for subsequent multi-objective optimization research.

Table 8. Error analysis of Kriging prediction model.

Design Objectives	MRE	R^2	$Radj^2$
y_1	0.0846	0.921	0.910
y_2	0.0695	0.952	0.945

By taking y_1 and y_2 as the optimization objectives, NSGA-II was used to perform a two-objective optimization solution using the Kriging prediction model. The population size was 40, the evolutionary algebra was 200, the hybridization probability was 0.8, the hybridization distribution index was 20, the mutation probability was 0.2, and the mutation distribution coefficient was 20. The Pareto frontier is obtained through 200 iterations, as shown in Figure 5a. Then, y_1, y_2, and y_3 were used as the optimization objectives, and y_4 was used as a constraint to perform a three-objective performance optimization on CSCPG. After 200 NSGA-II iterations, the Pareto front was obtained, as shown in Figure 5b,c.

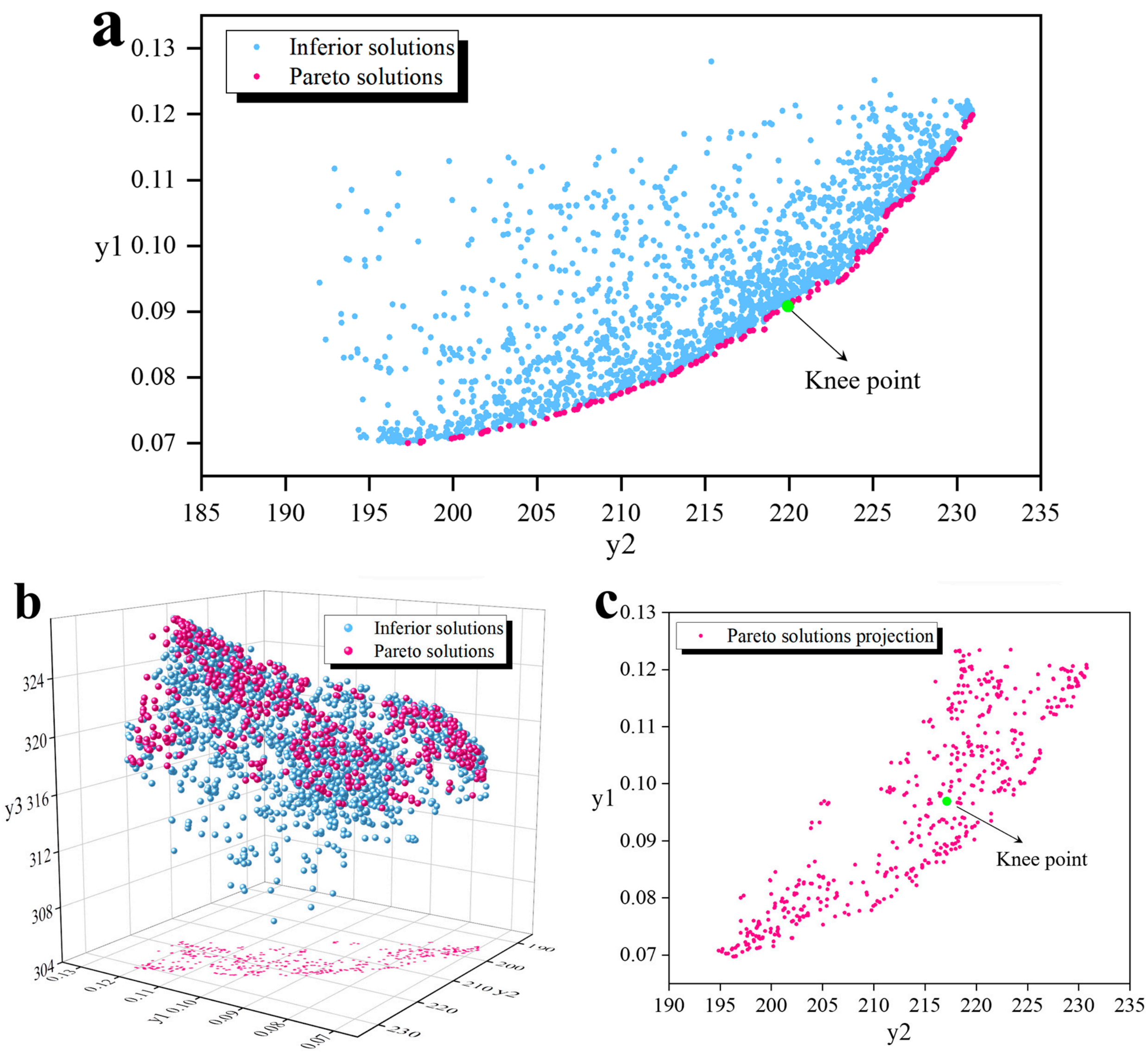

Figure 5. NSGA-II multi-objective optimization results. (**a**) Two-objective optimization solution; (**b**) Three-objective optimization solution; (**c**) projection of three-objective optimization solution in the y_1 and y_2 plane.

4. Results and Discussions

4.1. Analysis of Significant Influencing Factors

As shown in Figure 3a and Table 5, the analysis of the test results of USFD using the half-normal plot shows that the factors that have a significant impact on the friction coefficient of lubricating grease are the viscosity of the base oil and the content of nano-solid friction reducers. By combining this with Figure 4a, it can be seen that the friction coefficient decreases with the increase in nano-solid friction reducers content, reaching the minimum value when the content reaches about 1.5%, and then the friction coefficient begins to increase, which indicates that the addition of nano-solid friction reducers can effectively reduce the friction coefficient of lubricating grease. However, its content is not the best, which may be related to the increase in grease consistency caused by excessive nano-solid friction reducers. The friction coefficient decreases as the viscosity of the base oil decreases. This is because the thickness of the lubricating oil film is closely related to the viscosity of the base oil. The lower the viscosity of the base oil, the thinner the lubricating oil film formed between the friction pairs, which reduces the relative sliding friction resistance of the friction pairs; that is, it reduces the friction coefficient [34]. The content of the three thickeners in CSCPG has a relatively small impact on the friction coefficient, indicating that under boundary lubrication conditions, the main lubricating agents between the friction pairs are the base oil and nano-solid friction reducers.

As shown in Figure 3b and Table 5, the significant influencing factors on the service life of CSCPG are the content of polyurea thickener and antioxidants, as well as the thickening reaction temperature. As shown in Figure 4b,c, as the content of polyurea thickener and antioxidants increases, the service life of CSCPG increases. This is because the polyurea thickener does not contain metal ions, which avoids the catalytic effect of metal ions in the thickener on the oxidation of the lubricating grease base oil [35]. The addition of antioxidants has a better protective effect on the base oil, allowing CSCPG to remain non-oxidized for a longer period. As shown in Figure 4d, the service life of CSCPG first increases and then decreases with the increase in thickening reaction temperature. When the thickening reaction temperature reaches 125 °C, the service life of CSCPG reaches its maximum value, indicating that the optimal temperature for the thickening reaction is around 125 °C, which may be due to the increase in temperature accelerating the polymerization reaction that forms a thickener, but an excessively high temperature degrades the polyurea chains. As shown in Figure 5a, when y_1 and y_2 are used as optimization objectives, a set of Pareto solutions can be obtained. In Pareto solutions, the longer the service life of CSCPG, the greater the friction coefficient, with the lowest friction coefficient of 0.07. Currently, the service life of the lubricating grease is about 197 h, and the maximum service life of the lubricating grease can reach 230 h, with a friction coefficient of about 0.12. The shortest distance method [36] is adopted to find the optimal solution in Pareto solutions, which is to calculate the sum of the distances from each non-inferior solution to all other non-inferior solutions in all objective function spaces, and select the non-inferior solution with the shortest distance as the final optimal solution (knee point) for the problem. As shown in Figure 5b, when y_1, y_2, and y_3 are used as optimization objectives, a set of Pareto solutions in three-dimensional space can be obtained. By projecting these solutions onto the y_1 and y_2 planes, the knee point of Pareto solutions can be obtained (Figure 5c).

As shown in Table 9, when comparing the initial group with the two-objective optimization results (Optimal Prediction-II) and three-objective optimization results (Optimal Prediction-III), when y_1 and y_2 are used as optimization targets, the optimized friction coefficient can be reduced by up to 5.3% ((0.094 − 0.089)/0.094), and the service life can be increased by up to 3.8% ((220 − 212)/212). When y_1, y_2, and y_3 are used as optimization targets, the optimized droplet point can increase by up to 3.9% (322 − 310)/310), but its friction coefficient slightly increases compared to the initial group.

Table 9. Comparison of NSGA-II multi-objective optimization before and after.

	x_1	x_2	x_3	x_4	x_5	x_6	y_1	y_2	y_3
Initial group	26	150	8	2	1.5	130	0.094	212	310
Optimal Prediction-II	32	130	8	3	1.7	113	0.089	220	317
Optimal Prediction-III	34	143	8	2.7	1.5	103	0.097	217	322
Maximum optimization	-	-	-	-	-	-	5.3%	3.8%	3.9%

4.2. Optimization Analysis of Tribological Performance

As shown in Figure 6, The friction coefficient and standard deviation of the three groups of tribological tests are obtained with the initial group as the control group (CG), the two-objective optimization result as the optimal prediction 2 group (OP-2), and the three-objective optimization result as the optimal prediction 3 group (OP-3). After multi-objective optimization, the friction coefficient of OP-2 is the smallest (0.088). When compared with the predicted value (0.089), the relative error is only 1.1%, indicating that the prediction model has high accuracy. From the direction of the friction coefficient, all curves first increase, then gradually decrease, and tend to stabilize. After the friction coefficient reaches stability, it still fluctuates within a certain range. Among them, OP-2 has the smallest fluctuation, with a standard deviation of only 0.68×10^{-3}, indicating that the optimized CSCPG has improved friction reduction performance and its friction process is more stable.

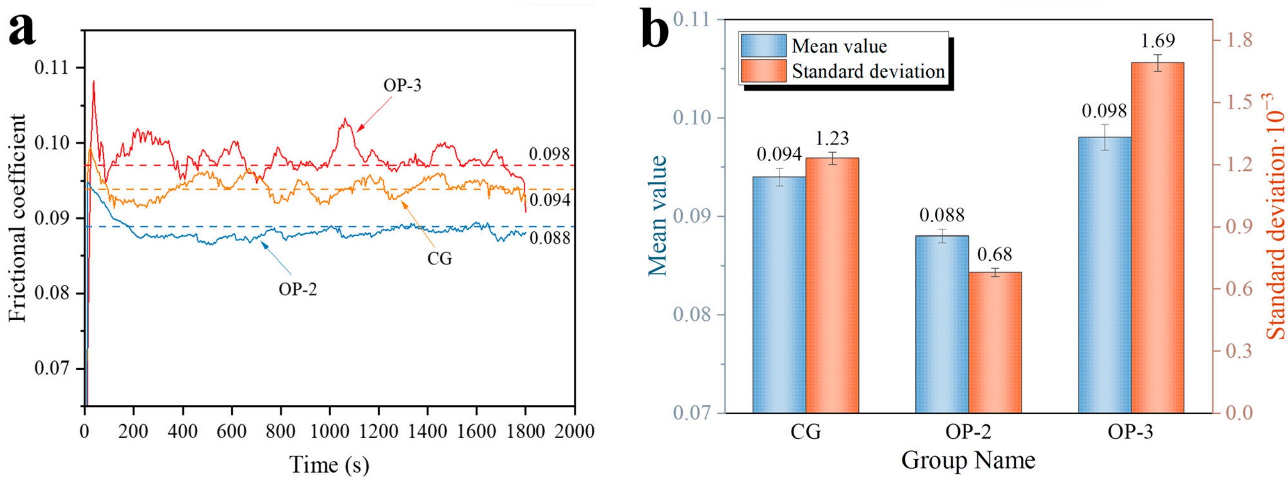

Figure 6. Tribological performance of CSCPG before and after optimization. (**a**) Dynamic curve of friction coefficient; (**b**) the average and standard deviation of the friction coefficient during the stable stage.

As shown in Figure 7, to further explore the wear situation of CSCPG on the surface of AISI E52100 steel after different optimizations, a three-dimensional optical profilometer (UP-3D, Rtec) is used to observe the surface morphology of the wear marks. Three sets of 3D maps and the surface roughness curves of the wear marks are obtained, as shown in Figure 7a,d,g. There are obvious wear marks on the surface of the three test samples, but the structural dimensions and surface characteristics of the wear marks are different. From the roughness of the wear marks, OP-2 has the smallest surface roughness and less surface damage, indicating that the CSCPG formulated by OP-2 can effectively lubricate and protect the surface of the friction pair [37]. OP-3 has the largest roughness along the direction of the wear marks (yellow line) and perpendicular to the direction of the wear marks (red line). From the roughness curve along the direction of the wear marks (Figure 7h), there are deep convex peaks and furrows on the surface of the wear marks, which indicates that the surface damage is relatively severe, and the lubrication performance of this formula CSCPG is poor.

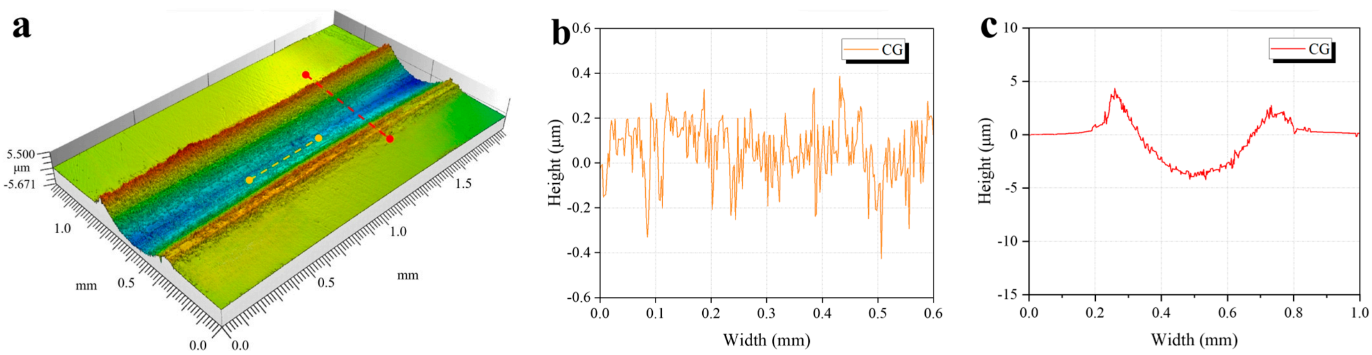

Figure 7. *Cont.*

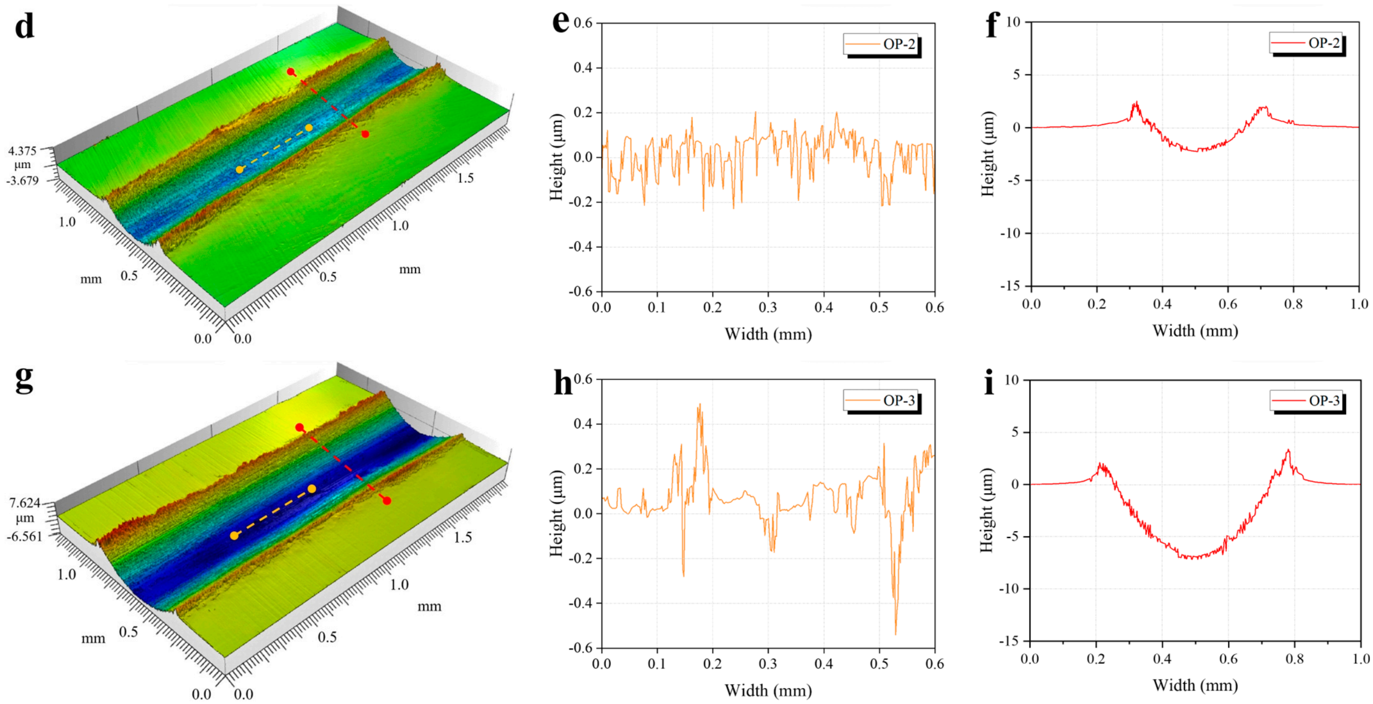

Figure 7. Three-dimensional maps, roughness along the direction of wear scars (yellow), and roughness of the cross-section (red) of the CSCPG wear marks before and after optimization. (**a**–**c**) CG; (**d**–**f**) OP-2; (**g**–**i**) OP-3.

As shown in Figure 8a, the wear scar width and depth of OP-2 after three sets of tribological tests are the smallest at 392 µm and 2.26 µm, respectively. When compared to CG, the wear scar width decreases by 14.2%, and the wear scar depth decreases by 46.3%. As shown in Figure 8b, OP-2 has the smallest wear volume and wear rate. When compared to CG, the wear volume decreases by 41.9%, and the wear rate decreases by 42.5%, indicating that the optimized CSCPG has a significantly enhanced wear resistance.

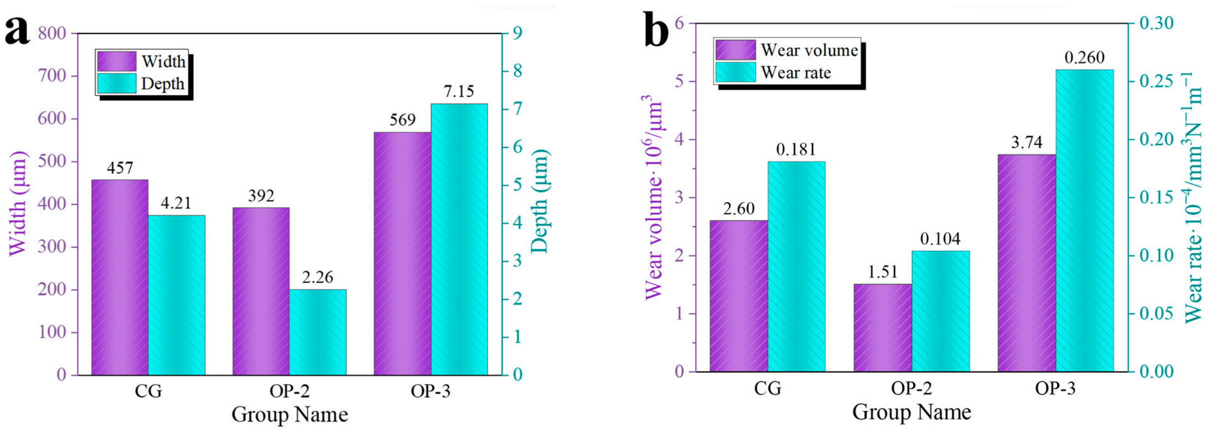

Figure 8. Wear performance of wear marks before and after optimization. (**a**) The width and depth of wear marks; (**b**) wear volume and wear rate of wear marks.

4.3. Optimization Analysis of Service Life

The service life results of the lubricating grease exhibit significant discreteness, as these data do not follow a normal distribution but follow a Weibull distribution [38,39]. Therefore, the distribution testing and parameter estimation of the Weibull distribution can be used to obtain the estimated values of the service life characteristics. When the experimental sample size is less than 25, the best linear unbiased estimation (BLUE) method is usually used to estimate the parameters of the Weibull distribution. As shown in Figure 9a–c, the service life data of the grease samples before and after optimization are all within the 95% confidence interval, indicating that the service life of the grease satisfies the Weibull distribution function. As shown in Figure 9d, the shape parameters (β) of the three grease samples are all >4, indicating that the distribution of the service life results of the lubricating grease represents a negative stress distribution, and the service life of the lubricating grease belongs to the attritional failure problems. Here, a 50% reliability service life (L_{50}) is selected as the estimated service life of CSCPG. The L_{50} service life of OP-2 is the highest at 222 h, with a relative error of only 0.9% when compared to the predicted value (220), indicating that the prediction model has high accuracy. When compared with CG, the L_{50} service life of OP-2 has increased by 4.7%, indicating that the optimization scheme can effectively extend the service life of CSCPG.

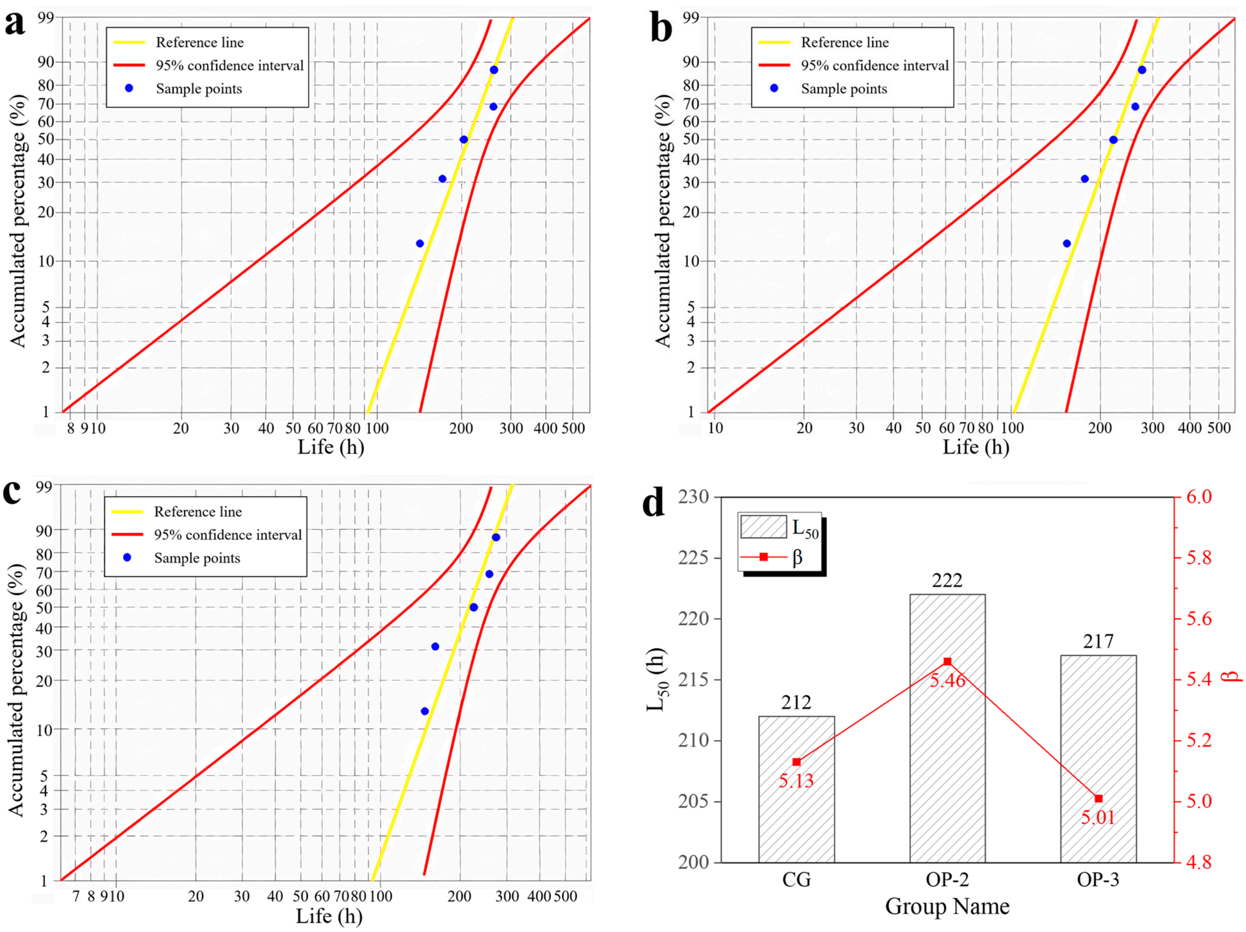

Figure 9. Comparison of the service life of CSCPG before and after optimization. (**a**) CG; (**b**) OP-2; (**c**) OP-3; (**d**) L_{50} service life and the shape parameter β.

5. Conclusions

This article screened out those factors that had a significant impact on the tribological performance and service life of CSCPG based on USFD. A Kriging prediction model for the tribological performance and service life of CSCPG was established based on the significant influencing factors. NSGA-II was used to optimize the production of raw materials and the preparation process of CSCPG. The tribological performance and service life of CSCPG before and after optimization were compared, and the following conclusions were obtained:

(1) The USFD method was used to screen those factors that may affect the tribological properties and service life of CSCPG during the preparation process. It was found that the viscosity of the base oil and the content of nano-solid friction reducers had a

significant impact on the tribological properties of CSCPG, whereas the content of the polyurea thickeners and antioxidants, as well as the thickening reaction temperature, had a significant impact on the service life of CSCPG;

(2) By optimizing the significant influencing factors of CSCPG through NSGA-II, a set of Pareto solutions can be obtained. When the friction coefficient and service life were used as the optimization objectives, the friction coefficient of the initial group of CSCPG could be reduced by 5.3%, and the service life could be extended by 3.8%. When increasing the droplet point as the third optimization objective, the friction coefficient increases;

(3) The results of the tribological and life tests indicate that the Kriging prediction model has high accuracy. When compared to the predicted results, the relative error of the friction coefficient is only 1.1%, and the relative error of the service life is only 0.9%. This can be used to guide the preparation and performance optimization of CSCPG.

Author Contributions: Conceptualization, H.Z. and Y.M.; Data curation, H.Z. and Y.M.; Formal analysis, H.Z. and Q.L. (Qingchun Liu); Funding acquisition, Y.M.; Investigation, Q.L. (Qingchun Liu) and J.W.; Methodology, H.Z. and Y.M.; Project administration, Q.L. (Qian Li); Resources, Q.L. (Qian Li); Software, H.Z. and Q.L. (Qingchun Liu); Supervision, Y.M.; Validation, H.Z., J.W. and Q.L. (Qian Li); Visualization, J.W.; Writing—original draft, H.Z.; Writing—review & editing, Y.M. All authors have read and agreed to the published version of the manuscript.

Funding: This research received no external funding.

Data Availability Statement: The data presented in this study are available in this article.

Conflicts of Interest: The authors declare no conflict of interest.

References

1. Allmaier, H. Increase Service Life for Rail Wheel Bearings—A Review of Grease Lubrication for This Application. *Lubricants* **2022**, *10*, 36. [CrossRef]
2. Bakunin, V.N.; Aleksanyan, D.R.; Bakunina, Y.N. Calcium Carbonate Polymorphs in Overbased Oil Additives and Greases. *Russ. J. Appl. Chem.* **2022**, *95*, 461–471. [CrossRef]
3. Sniderman, D. Calcium sulfonate complex greases. *Tribol. Lubr. Technol.* **2016**, *72*, 28.
4. Kobylyanskii, E.V.; Kravechuk, G.G.; Makedonskii, O.A.; Ishchuk, Y.L. Structure of ultrabasic sulfonate greases. *Chem. Technol. Fuels Oils* **2002**, *38*, 110–114. [CrossRef]
5. Fan, X.; Li, W.; Li, H.; Zhu, M.; Xia, Y.; Wang, J. Probing the effect of thickener on tribological properties of lubricating greases. *Tribol. Int.* **2018**, *118*, 128–139. [CrossRef]
6. Wen, Z.; Xia, Y.; Feng, X. Tribological Properties of the Overbased Calcium Sulfonate Complex Greases. In *Advanced Materials Research*; Zhao, H., Ed.; Mechanical and Electronics Engineering III, PTS 1-5; Trans Tech Publications, Ltd.: Zurich, Switzerland, 2012; Volume 130–134, pp. 891–894. [CrossRef]
7. Woo, J.; Lee, D.; Ryong, H.K. Studies on the synthesis and characteristics of calcium sulfonate complex grease. *J. Korea Acad.-Ind. Coop. Soc.* **2019**, *20*, 8–15. [CrossRef]
8. Liu, D.; Zhao, G.; Wang, X. Tribological Performance of Lubricating Greases Based on Calcium Carbonate Polymorphs Under the Boundary Lubrication Condition. *Tribol. Lett.* **2012**, *47*, 183–194. [CrossRef]
9. Gao, Y.; Ge, X.; Wen, Z.; Xia, Y. Comparison Friction and Wear Properties of Overbased Calcium Sulfonate Complex Grease and Polyurea Grease. In *Advanced Materials Research*; Wu, J., Lu, X., Xu, H., Nakagoshi, N., Eds.; Resources and Sustainable Development, PTS 1-4; Trans Tech Publications, Ltd.: Zurich, Switzerland, 2013; Volume 734–737, p. 2484. [CrossRef]
10. Zhang, H.; Mo, Y.M.; Lv, J.C.; Wang, J. Tribological Behavior of WS2 Nanoparticles as Additives in Calcium Sulfonate Complex-Polyurea Grease. *Lubricants* **2023**, *11*, 259. [CrossRef]
11. Wu, C.; Hong, Y.; Ni, J.; Teal, P.D.; Yao, L.; Li, X. Investigation of mixed hBN/Al_2O_3 nanoparticles as additives on grease performance in rolling bearing under limited lubricant supply. Colloid Surf. *A-Physicochem. Eng. Asp.* **2023**, *659*, 130811. [CrossRef]
12. Wu, C.; Liu, Z.; Ni, J.; Yang, K.; Yang, H.; Li, X. Improved tribological and bearing vibration performance of calcium sulfonate complex grease dispersed with MoS2 and oxide nanoparticles. *Proc. Inst. Mech. Eng. Part C-J. Eng. Mech. Eng. Sci.* **2023**, *237*, 1941–1955. [CrossRef]
13. Venkataramani, P.S.; Srivastava, R.G.; Gupta, S.K. High temperature greases based on polyurea gellants: A review. *J. Synth. Lubr.* **1987**, *4*, 229–244. [CrossRef]
14. Lyadov, A.S.; Maksimova, Y.M.; Ilyin, S.O.; Gorbacheva, S.N.; Parenago, O.P.; Antonov, S.V. Specific Features of Greases Based on Poly-alpha-olefin Oils with Ureate Thickeners of Various Structures. *Russ. J. Appl. Chem.* **2018**, *91*, 1735–1741. [CrossRef]

15. Maksimova, Y.M.; Shakhmatova, A.S.; Ilyin, S.O.; Pakhmanova, O.A.; Lyadov, A.S.; Antonov, S.V.; Parenago, O.P. Rheological and Tribological Properties of Lubricating Greases Based on Esters and Polyurea Thickeners. *Pet. Chem.* **2018**, *58*, 1064–1069. [CrossRef]
16. Liu, L.; Sun, H.W. Impact of polyurea structure on grease properties. *Lubr. Sci.* **2010**, *22*, 405–413. [CrossRef]
17. Ren, G.; Zhou, C.; Fan, X.; Zheng, M.; Wang, S. Investigating the rheological and tribological properties of polyurea grease via regulating ureido amount. *Tribol. Int.* **2022**, *173*, 107643. [CrossRef]
18. Ren, G.; Sun, X.; Li, W.; Li, H.; Zhang, L.; Fan, X.; Li, D.; Zhu, M. Improving the lubrication and anti-corrosion performance of polyurea grease via ingredient optimization. *Friction* **2021**, *9*, 1077–1097. [CrossRef]
19. Cyriac, F.; Lugt, P.M.; Bosman, R. Impact of Water on the Rheology of Lubricating Greases. *Tribol. Lubr. Technol.* **2017**, *73*, 56–70. [CrossRef]
20. Zhou, Y.; Bosman, R.; Lugt, P.M. On the Shear Stability of Dry and Water-Contaminated Calcium Sulfonate Complex Lubricating Greases. *Tribol. Trans.* **2019**, *62*, 626–634. [CrossRef]
21. Bosman, R.; Lugt, P.M. The Microstructure of Calcium Sulfonate Complex Lubricating Grease and Its Change in the Presence of Water. *Tribol. Trans.* **2018**, *61*, 842–849. [CrossRef]
22. Sun, L.; Ma, R.; Zhao, Q.; Zhao, G.; Wang, X. The Impact of Water on the Tribological Behavior of Lubricating Grease Based on Calcium Carbonate Polymorphs. *Lubricants* **2022**, *10*, 188. [CrossRef]
23. Cyriac, F.; Lugt, P.M.; Bosman, R.; Venner, C.H. Impact of Water on EHL Film Thickness of Lubricating Greases in Rolling Point Contacts. *Tribol. Lett.* **2016**, *61*, 23. [CrossRef]
24. Xu, J.; Wang, P.; Ma, X.; Qian, Y.; Chen, R. Parameters studies for rail wear in high-speed railway turnouts by unreplicated saturated factorial design. *J. Cent. South Univ.* **2017**, *24*, 988–1001. [CrossRef]
25. Hou, S.; Dong, D.; Ren, L.; Han, X. Multivariable crashworthiness optimization of vehicle body by unreplicated saturated factorial design. *Struct. Multidiscip. Optim.* **2012**, *46*, 891–905. [CrossRef]
26. Kleijnen, J. Kriging metamodeling in simulation: A review. *Eur. J. Oper. Res.* **2009**, *192*, 707–716. [CrossRef]
27. Deb, K.; Pratap, A.; Agarwal, S.; Meyarivan, T. A fast and elitist multiobjective genetic algorithm: NSGA-II. *IEEE Trans. Evol. Comput.* **2002**, *6*, 182–197. [CrossRef]
28. Li, H.; Zhang, Q.F. Multiobjective Optimization Problems with Complicated Pareto Sets, MOEA/D and NSGA-II. IEEE Trans. *Evol. Comput.* **2009**, *13*, 284–302. [CrossRef]
29. Ren, G.; Zhang, P.; Li, W.; Fan, X.; Zhang, L.; Li, H.; Zhu, M. Probing the Synergy of Blended Lithium Complex Soap and Calcium Sulfonate Towards Good Lubrication and Anti-Corrosion Performance. *Tribol. Lett.* **2020**, *68*, 99. [CrossRef]
30. Qi, P.; Wang, S.; Li, J.; Li, Y.; Dong, G. Synergistic lubrication effect of antioxidant and low content ZDDP on PFPE grease. *Ind. Lubr. Tribol.* **2021**, *73*, 830–838. [CrossRef]
31. Dai, X.Z.; Guo, P.; Hong, D.M.; Hui, J.D.; Hui, Z.M.; Geng, F. The effect of preparation and characterisation of polyurea grease. *Mater. Res. Innov.* **2015**, *19*, 588–591. [CrossRef]
32. Jang, D.; Anderson-Cook, C.M. Examining robustness of model selection with half-normal and LASSO plots for unreplicated factorial designs. *Qual. Reliab. Eng. Int.* **2017**, *33*, 1921–1928. [CrossRef]
33. Skrypnyk, R.; Ekh, M.; Nielsen, J.C.O.; Palsson, B.A. Prediction of plastic deformation and wear in railway crossings—Comparing the performance of two rail steel grades. *Wear* **2019**, *428*, 302–314. [CrossRef]
34. Garshin, M.V.; Porfiryev, Y.V.; Zaychenko, V.A.; Shuvalov, S.A.; Kolybelsky, D.S.; Gushchin, P.A.; Vinokurov, V.A. Effect of Base Oil Composition on the Low-Temperature Properties of Polyurea Greases. *Pet. Chem.* **2017**, *57*, 1177–1181. [CrossRef]
35. Knothe, G.; Steidley, K.R. The effect of metals and metal oxides on biodiesel oxidative stability from promotion to inhibition. *Fuel Process. Technol.* **2018**, *177*, 75–80. [CrossRef]
36. Sanchez-Gomez, J.M.; Vega-Rodriguez, M.A.; Perez, C.J. Comparison of automatic methods for reducing the Pareto front to a single solution applied to multi-document text summarization. *Knowl.-Based Syst.* **2019**, *174*, 123–136. [CrossRef]
37. Wang, Z.; Xia, Y.; Liu, Z. The rheological and tribological properties of calcium sulfonate complex greases. *Friction* **2015**, *3*, 28–35. [CrossRef]
38. Zhang, F.S.; Liu, T.T.; Liu, J.T.; Cui, F.K. Research on Bearing Life Prediction Based on Three Parameters Weibull Distribution. In *Advanced Materials Research*; Zuo, D., Guo, H., Xu, H.L., Su, C., Liu, C.J., Jin, W., Eds.; Frontier in Functional Manufacturing Technologies; Trans Tech Publications, Ltd.: Zurich, Switzerland, 2010; Volume 136, pp. 162–166. [CrossRef]
39. Poplawski, J.V.; Peters, S.M.; Zaretsky, E.V. Effect of roller profile on cylindrical roller bearing life prediction—Part I: Comparison of bearing life theories. *Tribol. Trans.* **2001**, *44*, 339–350. [CrossRef]